

Description of our cosmological spacetime as a perturbed conformal Newtonian metric and implications for the backreaction proposal for the accelerating universe

Edward W. Kolb*

*Department of Astronomy and Astrophysics, Enrico Fermi Institute,
and Kavli Institute for Cosmological Physics, the University of Chicago, Chicago, IL 60637-1433, USA*

Valerio Marra†

*Dipartimento di Fisica “G. Galilei” Università di Padova,
INFN Sezione di Padova, via Marzolo 8, Padova I-35131, Italy and
Kavli Institute for Cosmological Physics, the University of Chicago, Chicago, IL 60637-1433, USA*

Sabino Matarrese‡

*Dipartimento di Fisica “G. Galilei” Università di Padova,
INFN Sezione di Padova, via Marzolo 8, Padova I-35131, Italy*

It has been argued that the spacetime of our universe can be accurately described by a perturbed conformal Newtonian metric, and hence even large density inhomogeneities in a dust universe can not change the observables predicted by the homogeneous dust model. In this paper we study a spherically symmetric dust model and illustrate conditions under which large spatial variations in the expansion rate can invalidate the argument.

PACS numbers: 98.80.-k, 95.36.+x

I. INTRODUCTION

In cosmology, one models the evolution and observables associated with an inhomogeneous universe of density $\rho(\vec{x})$ and expansion rate $H(\vec{x})$ by employing a Friedmann-Lemaître-Robertson-Walker (FLRW) homogeneous/isotropic model of density $\rho = \langle \rho(\vec{x}) \rangle$, where $\langle \cdots \rangle$ denotes some suitably defined spatial average. One then assumes that the expansion rate and cosmological observables are those obtained in the corresponding FLRW model.

One of the proposals to explain “dark energy” calls into question this long-standing (86-year) procedure. The idea is that the expansion rate and cosmological observables of a suitably inhomogeneous universe containing only dust, if analyzed within the framework of a homogeneous model, seems to behave as if the stress tensor also contains a fictitious negative-pressure fluid (*i.e.*, dark energy).

Although this proposal is conservative in the sense that it does not involve a cosmological constant of incredibly small magnitude (presumably rationalized on some anthropic basis), a scalar field of unbelievably small mass, or an entirely unmotivated modification of general relativity, it is rather revolutionary because it implies that there is no dark energy and the expansion of the universe does not actually accelerate (at least, not in the usual sense).

At present, the idea that the backreaction¹ of inhomogeneities accounts for the observational evidence usually attributed to dark energy is more of a concept than a predictive model. However, it is generally agreed that if the proposal is to be relevant, nonlinearities are required.

There have been many criticisms of this approach. One of them [1, 2] is based on the claim that even in the presence of highly nonlinear density perturbations ($\delta\rho/\rho \gg 1$) the metric for our universe can everywhere be written as a perturbed conformal Newtonian metric of the form²

$$ds^2 = a^2(\tau) \left[-(1 + 2\psi)d\tau^2 + (1 - 2\psi)\gamma_{ij}dx^i dx^j \right], \quad (1)$$

where $d\tau = dt/a$ is conformal time, γ_{ij} is a metric of a three-space of constant curvature, and ψ satisfies the Newtonian

*Electronic address: rocky.kolb@uchicago.edu

†Electronic address: valerio.marra@pd.infn.it

‡Electronic address: sabino.matarrese@pd.infn.it

¹ By the backreaction idea we mean both that inhomogeneities influence cosmological observables (weak backreaction) and that inhomogeneities influence the average/background scale factor (strong backreaction). Weak and strong backreactions are, however, likely connected if we assume that averages should be performed along the light cone.

² We will refer to a metric written in the form of Eq. (1), satisfying the stated conditions, as the *perturbed conformal Newtonian* metric.

conditions $|\psi| \ll 1$, $|\partial\psi/\partial t|^2 \ll a^{-2}D^i\psi D_i\psi$, and $(D^i\psi D_j\psi)^2 \ll (D^i D^j\psi) D_i D_j\psi$. The covariant derivative with the metric γ_{ij} is denoted by D_i . The usual statement is that in the dust case one is allowed to use the perturbed conformal Newtonian metric either in the linear regime (*i.e.*, perturbations of every quantity being small) or in the weak-field (Newtonian) regime.³

The claim is that if the metric can be written in the above form and satisfies the above conditions, even in the presence of large inhomogeneities, any cosmological observable will be the same as the cosmological observable calculated with $\psi = 0$, *i.e.*, in the homogeneous/isotropic model. This has been described as a “no-go” theorem that backreactions can not *in principle* account for the observations.

While it is impossible to consider the most general inhomogeneous solutions, there are spherically symmetric inhomogeneous dust solutions, which are not perturbations of Einstein-de Sitter, that can be constructed to give observables similar to Λ CDM models. These models serve as a counterexample to the no-go argument. In this paper we will show why these models can not be described in terms of a conformal Newtonian metric perturbed about a spatially flat background, and attempt to understand the implications for the backreaction proposal.

Indeed, while it may turn out that backreactions are not the answer, we argue that assuming the results of measurements of the luminosity distance as a function of redshift usually interpreted as an accelerated expansion, the metric describing our universe can not be written in the form of a perturbed conformal Newtonian metric where $a(t)$ is calculated from the homogeneous dust model. In other words, if the expansion history of the universe is well described by the Λ CDM model, then perturbing about an Einstein-de Sitter model by the perturbed conformal Newtonian metric of Eq. (1) is inappropriate, because Einstein-de Sitter would be the wrong background. This is because of large peculiar velocities with respect to the background Einstein-de Sitter space. So if inhomogeneities are responsible for the observables usually attributed to dark energy, the universe can not be obtained by small perturbations of the Einstein-de Sitter model. In other words, the reason we interpret the observations as evidence for dark energy and acceleration of the universe is that we are comparing the observables to observables computed in the wrong background.

As we will discuss, the reason is that the proper meaning of “peculiar” is “after subtraction of a background Hubble flow term.” We will argue that large peculiar velocities must be present if the backreaction program works, and the peculiar velocities are not related to “local” departures from the Hubble flow that would show up as large velocity dispersions.

As an explicit example, consider the argument of Ref. [3]. They propose that the backreaction of inhomogeneities in a dust universe modifies the evolution of the effective volume-averaged scale factor and results in an evolution of the volume expansion that resembles a Λ CDM model, rather than the unperturbed spatially flat dust model. If one would write the metric for such a perturbed universe in terms of a perturbed conformal Newtonian metric, then one would have to use $a(t)$ described by a Λ CDM model, *not* the $a(t)$ from an unperturbed spatially flat dust model. If one would attempt to express the metric in terms of a perturbed metric with $a(t)$ described by a spatially flat dust model, then there would be enormous peculiar velocities in the Hubble flow.

We explore the issue by considering the spacetime of a particular Lemaître-Tolman-Bondi spherically symmetric model. In the model we study, the observer is centered in a large (Gpc) underdense region in an asymptotically Einstein-de Sitter universe. This model has large, but not highly nonlinear, density and curvature inhomogeneities. We show by explicit calculation that the metric *can not* be expressed as a perturbed conformal Newtonian metric during the entire evolution. We also show that the reason for this can be traced to large peculiar velocities that develop with respect to the Einstein-de Sitter background.

In the next Section we describe the relevant features of the Einstein-de Sitter and Lemaître-Tolman-Bondi models. In Section III we develop the formalism to express the original Lemaître-Tolman-Bondi metric in the form of a perturbed conformal Poisson metric. In Section IV we discuss the reason for the numerical results of the previous Section. Finally, in Section V we present our conclusions.

II. EINSTEIN-DE SITTER (EDS) AND LEMAÎTRE-TOLMAN-BONDI (LTB) MODELS

In this Section we will establish the notation for the homogeneous, isotropic, and spatially-flat cosmological model (the Einstein-de Sitter model). We will then briefly introduce the formalism of LTB spherically symmetric cosmological models in the synchronous gauge, and turn to a particular LTB model with values of cosmological observables similar to the Λ CDM model.

³ But already at second order in perturbation theory the spatial part of the metric differs from the temporal part of the metric simply from terms quadratic in the peculiar velocities (*i.e.*, an effective anisotropic stress term is in the stress-energy tensor).

A. The EdS model

The EdS model describes a spatially-flat, matter-dominated universe. In order to connect with the LTB solution of the next section, we can express the line element in terms of the scale factor $a(t)$:

$$ds^2 = -dt^2 + a^2(t)dr^2 + a^2(t)r^2 d\Omega^2. \quad (2)$$

The Friedmann equation and its solutions are (a_0 is the present scale factor—in general, the subscript 0 will denote the present value of a quantity and $\kappa = 8\pi G$)

$$\begin{aligned} H^2(t) &= (\dot{a}/a)^2 = \kappa\rho(t)/3 = H_0^2(a_0/a)^3 \\ a(t) &= a_0 (t/t_0)^{2/3} \\ \rho(t) &= \rho_0(a_0/a)^3. \end{aligned} \quad (3)$$

At any epoch, the age of the universe is $t = 2H^{-1}/3$. We also note that the present distance to the horizon is $d_H = 2H_0^{-1}$.

B. The LTB model

The LTB model [4, 5, 6] is based on the assumptions that the system is spherically symmetric with purely radial motion and the motion is geodesic without shell crossing (otherwise we could not neglect the pressure). The line element in the synchronous gauge can be written in the form

$$ds^2 = -dt^2 + \frac{R'^2(r, t)}{W^2(r)} dr^2 + R^2(r, t) d\Omega^2. \quad (4)$$

Here, the prime superscript denotes d/dr . We will denote d/dt by an overdot. The function $W(r)$ is an arbitrary function of r . We will also find it useful to define equivalent functions $\beta(r)$ and $k(r)$, related to $W(r)$ by

$$W^2(r) = 1 + \beta(r) = 1 - k(r)r^2. \quad (5)$$

One can recover the usual Friedmann-Robertson-Walker metric by the replacements

$$\begin{aligned} R(r, t) &\rightarrow ra(t) \\ k(r) &\rightarrow \pm 1, \text{ or } 0. \end{aligned} \quad (6)$$

In spherically symmetric models, in general there are two expansion rates: an angular expansion rate, $H_\perp \equiv \dot{R}(r, t)/R(r, t)$, and a radial expansion rate, $H_r \equiv \dot{R}'(r, t)/R'(r, t)$.

Assuming a dust equation of state, the Einstein equations may be expressed as

$$\begin{aligned} H_\perp^2 + 2H_r H_\perp - \frac{\beta}{R^2} - \frac{\beta'}{RR'} &= \kappa\rho \\ 6\frac{\ddot{R}}{R} + 2H_\perp^2 - 2\frac{\beta}{R^2} - 2H_r H_\perp + \frac{\beta'}{RR'} &= -\kappa\rho. \end{aligned} \quad (7)$$

These are the generalization of the Friedmann equations for a homogeneous/isotropic universe to a spherically symmetric inhomogeneous universe.

Adding the equations results in an equation that can be easily integrated to yield the dynamical equation for $R(r, t)$:

$$\dot{R}(r, t) = \sqrt{\beta(r) + \frac{\alpha(r)}{R(r, t)}}, \quad (8)$$

where $\alpha(r)$ is a function of r related to the density $\rho(r, t)$ by

$$\kappa\rho(r, t) = \frac{\alpha'(r)}{R^2(r, t)R'(r, t)}. \quad (9)$$

Equation (8) can be differentiated to yield the dynamical equation for $R'(r, t)$:

$$\dot{R}'(r, t) = \frac{\beta'(r) + \alpha'(r)/R(r, t) - \alpha R'(r, t)/R^2(r, t)}{2\dot{R}(r, t)}. \quad (10)$$

Since we will eventually express the LTB solution using a perturbed conformal Poisson metric, it is convenient to use instead of time a new independent variable related to the EdS scale factor: $x = a/a_0$. We also introduce new dependent variables $Y = R/ar$ and $Z = R'/a$. Therefore, our variables are

$$\begin{aligned} x &= \frac{a}{a_0} \\ Y(x, r) &= \frac{R}{ar} \\ Z(x, r) &= \frac{R'}{a}. \end{aligned} \quad (11)$$

The solution $Y = Z = 1$ corresponds to the EdS model. The dynamical equations for Y and Z are

$$\begin{aligned} \frac{dY}{dx} &= \frac{Y}{x} \left[\sqrt{\frac{B_1 x}{Y^2} + \frac{A_1}{Y^3}} - 1 \right] \\ \frac{dZ}{dx} &= \frac{Z}{x} \left[\frac{1}{2Z} \frac{x B_2 + A_2/Y - A_1 Z/Y^2}{\sqrt{B_1 x + A_1/Y}} - 1 \right], \end{aligned} \quad (12)$$

where the functions $A_1(r)$, $A_2(r)$, $B_1(r)$, and $B_2(r)$ are related to $\alpha(r)$, $\beta(r)$ and their derivatives by

$$\begin{aligned} \alpha(r) &= H_0^2 a_0^3 r^3 A_1(r) \\ \alpha'(r) &= H_0^2 a_0^3 r^2 A_2(r) \\ \beta(r) &= H_0^2 a_0^2 r^2 B_1(r) \\ \beta'(r) &= H_0^2 a_0^2 r B_2(r). \end{aligned} \quad (13)$$

Here, $H_0 = H_\perp(t_0, r \rightarrow \infty) = H_r(t_0, r \rightarrow \infty) = 100 h \text{ km s}^{-1} \text{ Mpc}^{-1}$ is the present EdS expansion rate.

Since each shell labeled by r evolves independently, we can choose initial conditions to be specified at different times for different shells. However, for simplicity we choose to specify initial conditions at the same time for all shells. We will choose the initial time to be recombination for the EdS model, $x^{-1} = 1100$. The initial value of R (or Y) can be chosen freely with a suitable rescaling of r . We choose $Y = Z = 1$ at $x^{-1} = 1100$ to match to the EdS solution as $r \rightarrow \infty$.

A particular LTB model is generated by a choice for $\alpha(r)$ and $\beta(r)$. For a discussion of the free functions in LTB models, see Ref. [7]. For other works based on LTB solutions aiming at showing the effect of inhomogeneities, see [7, 8, 9, 10, 11, 12, 13, 14, 15, 16, 17, 18, 19, 20, 21]. Our goal here is to study a LTB model with observables similar to the standard Λ CDM model. We will adopt the particular model of Alnes, Amarzguioui, and Grøn (AAG) [22, 23, 24], but with slightly different parameters. The model is EdS at large r , the observer is in the center of an underdense (compared to the EdS density) region, and there is a region of density larger than the EdS value to compensate the underdense region.

In the AAG model $\alpha(r)$ and $\beta(r)$ are given by

$$\begin{aligned} \alpha(r) &= H_0^2 a_0^3 r^3 \left[1 - \frac{\Delta\alpha}{2} \left(1 - \tanh \frac{r - r_0}{2\Delta r} \right) \right] \\ \beta(r) &= H_0^2 a_0^2 r^2 \frac{\Delta\alpha}{2} \left(1 - \tanh \frac{r - r_0}{2\Delta r} \right). \end{aligned} \quad (14)$$

Alnes, Amarzguioui, and Grøn choose $h = 0.51$, $\Delta\alpha = 0.9$, $a_0 r_0 = 1.35 \text{ Gpc}$, $\Delta r = 0.4 r_0$. With that choice of parameters, at the origin at present $h_\perp = h_r = 0.65$. They found that this choice of parameters reproduces the luminosity distance–redshift diagram expected for a Λ CDM model. That choice of parameters results in a “weak” singularity at the origin [12], as can be seen by the fact that $\rho'(r = 0) \neq 0$.⁴ While this is not a serious issue (the

⁴ What Ref. [12] actually claims is that if there is no weak singularity at the center, then for an observer at the center, $d\Delta(m - M)/dz$ cannot be positive at $z = 0$. However, it is possible to have $d\Delta(m - M)/dz > 0$ for off-center observers.

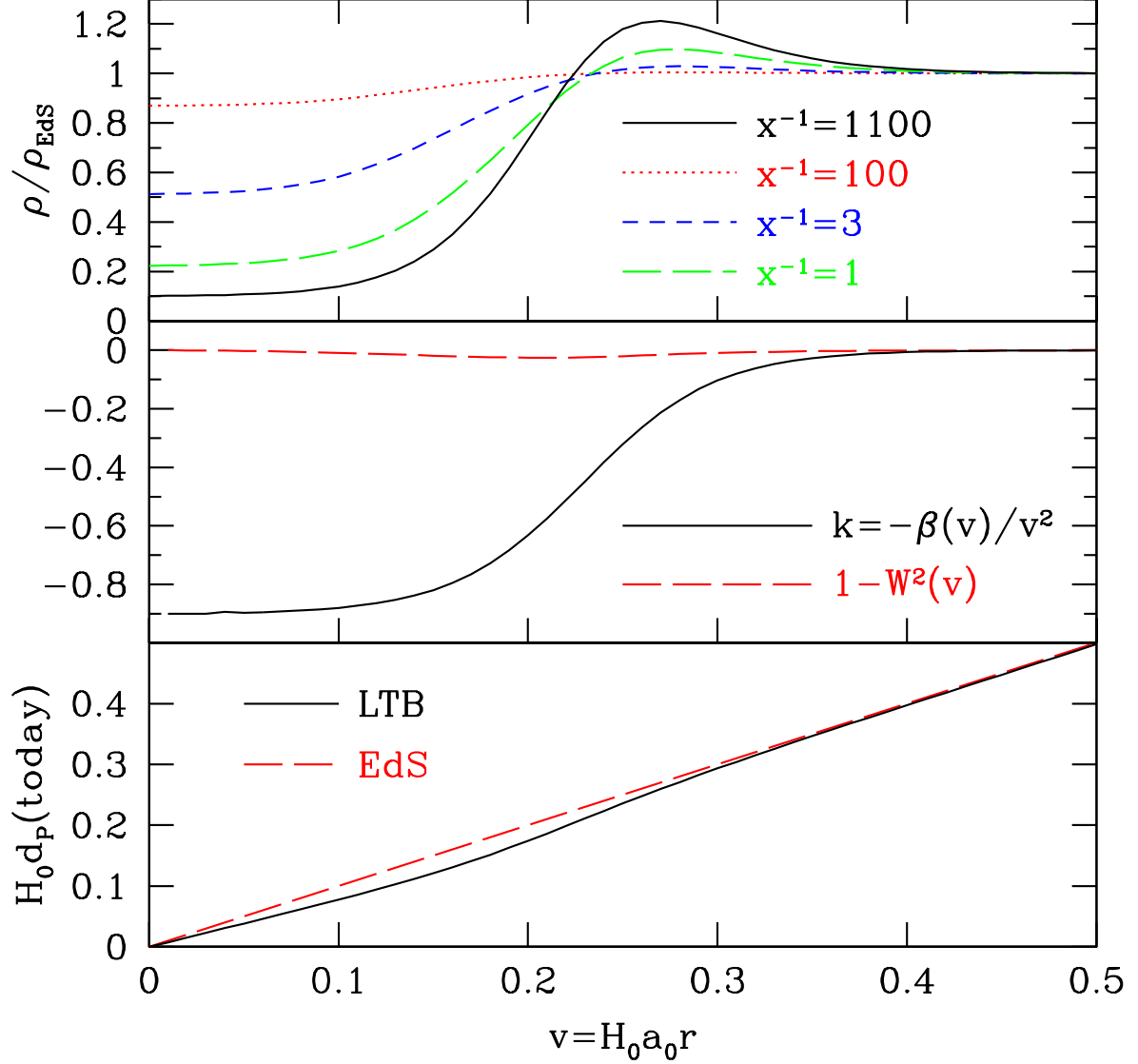


FIG. 1: Upper figure: The density compared to the density of the EdS model as a function of $v = H_0 a_0 r$ for various values of $x = a/a_0$. Middle figure: The functions $k = -\beta(v)/v^2$ and $-\beta(v) = 1 - W^2(v)$ as a function of $v = H_0 a_0 r$. Notice that W^2 is always very close to unity (an approximation we will employ later). Bottom figure: The current proper distance as a function of the comoving coordinate $v = H_0 a_0 r$ for the LTB model and the EdS model ($H_0^{-1} = 5878 \text{Mpc}$).

observer could be slightly displaced from the origin or a slightly different density profile could be used) we will employ different parameters than AAG to mitigate the weak singularity. We do this simply by the choice $\Delta r = 0.15 r_0$. This results in the present expansion rate at the origin of $h_{\perp} = h_r = 0.67$.

The density compared to the EdS density is shown in Fig. 1. Notice that at the origin ρ' vanishes. The curvature function $k(r)$ is also shown in Fig. 1. The fact that as r approaches 0, k is negative and ρ is much smaller than the EdS value, implies that the evolution deep in the void will resemble a negatively-curved, empty universe. For sufficiently large r , k approaches 0 and ρ approaches the EdS value, so far from the void the universe evolves as an

EdS model universe.⁵ The AAG model can actually be thought of as a swiss-cheese model of holes of radius v_{EdS} . (See Ref. [7] for a discussion of swiss-cheese models.)

In Fig. 1 we display the functions in term of the comoving coordinate label r multiplied by $H_0 a_0$. That combination is related to the present comoving proper distance in units of H_0^{-1} ,

$$H_0 d_P(\text{today}) = H_0 \int_0^r \frac{R'(r_1, t_0)}{W(r_1)} dr_1 = H_0 a_0 \int_0^r \frac{Z(x=1, r_1)}{W(r_1)} dr_1 = \int_0^v \frac{Z(x=1, v_1)}{W(v_1)} dv_1, \quad (15)$$

where $v \equiv H_0 a_0 r$. The spatial curvature term $W(r)$ is close to unity, and Z is of order unity, so to a reasonable approximation $H_0 d_P(\text{today}) = v$, the EdS result. (The choice $h = 0.51$ implies $H_0^{-1} = 5878$ Mpc.) In Fig. 1 we show the present proper distance as a function of $v = H_0 a_0 r$.

The evolution of $Y(x)$ and $Z(x)$ is shown in Fig. 2. The initial conditions specified at $x^{-1} = 1100$ are $Y = Z = 1$, with an initial underdensity in the interior. Since the underdense region expands more rapidly than average, a typical LTB evolution will lead to shell crossing in a rather small dynamical time. The occurrence of shell crossing means that the synchronous coordinate system becomes singular and the evolution in that system can no longer be calculated. AAG delay the onset of shell crossing by endowing the shells with a large initial infall velocity (negative dY/dx and dZ/dx). Thus, it takes the system a while for the underdense regions with large expansion rate to reverse the infall and this essentially delays the eventual shell crossing.⁶

Alnes, Amarazguoui, and Grøn also calculate the luminosity distance as a function of redshift, assuming that the observer is in the center of the underdense region ($r = 0$). The photon geodesic equation for the position of the photon as a function of time, $\hat{t}(r)$ or $\hat{x}(r)$, is found from the LTB metric [22]:

$$\frac{d\hat{t}}{dr} = -\frac{R'(r, \hat{t})}{\sqrt{1 + \beta(r)}} \rightarrow \frac{d\hat{x}}{dv} = -\hat{x}^{1/2} \frac{Z(\hat{x}, v)}{W(v)}, \quad (16)$$

where we have used the new comoving radial coordinate $v = H_0 a_0 r$. The redshift of the photon, $z(r)$ or $z(v)$, is [10, 22]

$$\frac{dz}{dr} = (1 + z) \frac{\dot{R}(r, \hat{t})}{\sqrt{1 + \beta(r)}} \rightarrow \frac{dz}{dv} = \frac{1 + z}{\hat{x}^{1/2}} \frac{Z(\hat{x}, v)}{W(v)} \left(1 + \frac{\hat{x}}{Z(\hat{x}, v)} \frac{dZ(\hat{x}, v)}{d\hat{x}} \right). \quad (17)$$

Equations (16) and (17) are solved with initial conditions $z = v = 0$ at $x = 1$. The luminosity distance is then simply

$$d_L(z) = (1 + z)^2 R(r, \hat{t}) \rightarrow H_0 d_L(z) = (1 + z)^2 \hat{x} v Y(\hat{x}, v). \quad (18)$$

A graph of the luminosity distance as a function of redshift is shown in Fig. 3. The striking feature in Fig. 3 is that the LTB model resembles a dark-energy model. AAG show that their LTB model is a better fit to the “gold” data set of Riess *et al.* [25] than the concordance Λ CDM model (at the expense of additional parameters). With our different choice for Δr , $d_L(z)$ in our model is slightly different than the AAG choice of parameters, but nevertheless demonstrates a shape characteristic of Λ CDM models. Note that as $z \rightarrow 0$, $d_L(z)$ follows the curve expected for the empty model. This is because the center of the void *is*, in fact, evolving as an empty universe at late times.

Whether our (or AAG’s) LTB model is a better fit than Λ CDM in light of new data is inconsequential. Our goal is not to champion any particular LTB model as a cosmological model that describes our universe, but rather to explore the failure of the no-go argument that inhomogeneities can not describe $d_L(z)$ because the spacetime of our universe can be expressed in the perturbed Newtonian form.

We note that in the LTB model there is no dark energy, and since there is only a pressureless component to the stress-tensor, no individual fluid element undergoes local acceleration.

We emphasize that observations can not directly establish that there is dark energy, or even that the universe accelerates in the usual sense. They only tell us that high-redshift supernovae are about one-half magnitude fainter than expected in the Einstein-de Sitter model. Stronger statements have additional (always unstated) model assumptions!

In the next section we will discuss the formulation of the model using a perturbed conformal Poisson metric. But before turning to the main issue of this paper, we note that although no fluid element in the LTB model undergoes local acceleration, one can easily show that in the backreaction proposal a suitably volume-averaged definition of the scale factor has negative pressure (see Refs. [3, 18, 26, 27, 28, 29, 30] for a discussion). This is related to the averaging issue in cosmology as emphasized by Buchert and Ellis [31, 32].

⁵ We will refer to the value of r or v when the solution is very near the EdS solution as r_{EdS} or v_{EdS} .

⁶ As far as the purpose of this model is concerned (having observables similar to the Λ CDM model), the synchronous gauge does not have problems, and, in particular, the LTB solution is an exactly solvable model with nonlinear inhomogeneities for an extended time evolution.

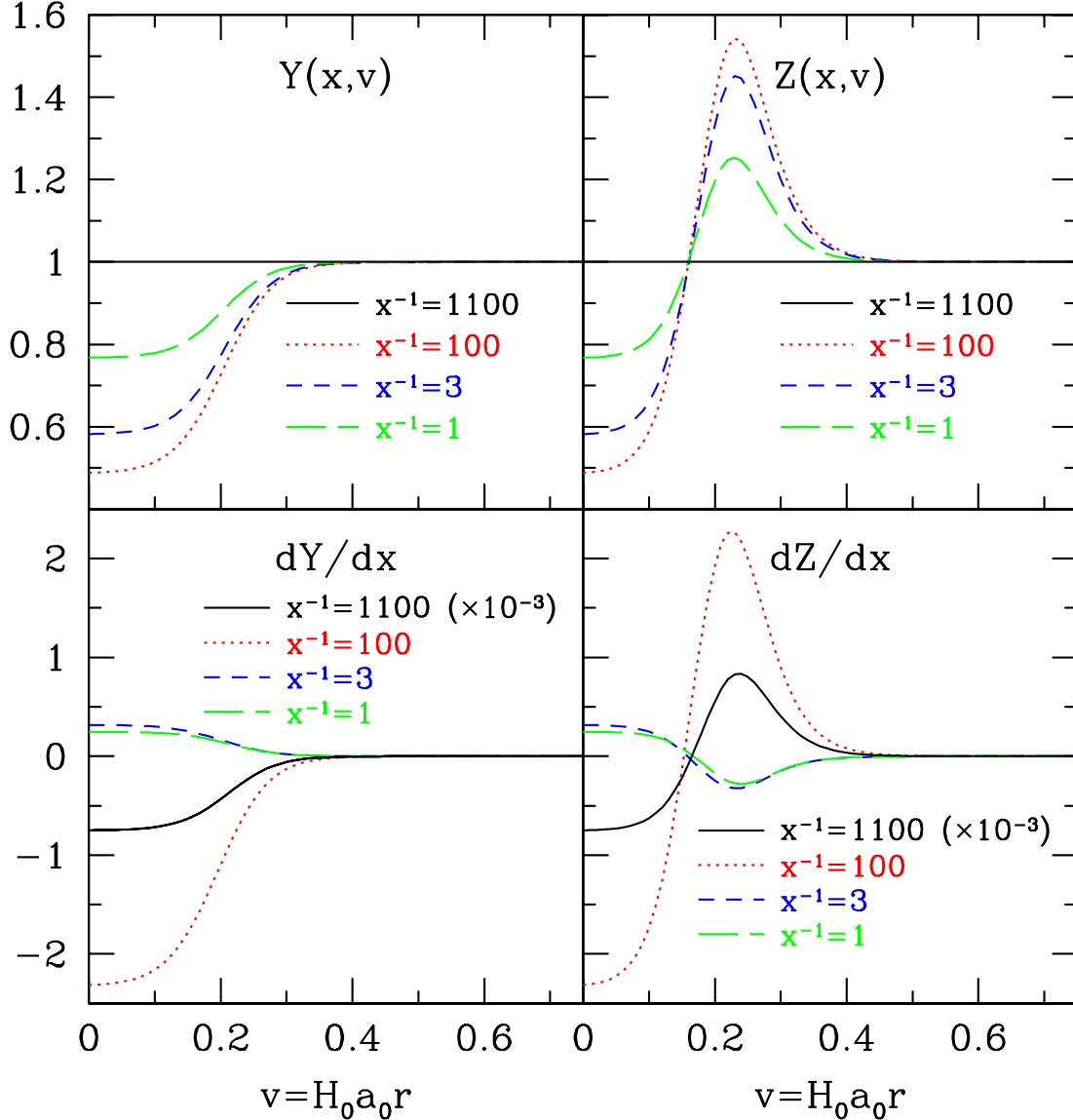


FIG. 2: Upper figures: The functions Y and Z as a function of $v = H_0 a_0 r$ for the indicated values of $x = a/a_0$. At the initial time of the evolution, $x^{-1} = 1100$ and $Y = Z = 1$. For the other values of x , Y is always smaller than unity and asymptotically approaches $Y = 1$ (the EdS solution) for large values of v . For small values of v the function Z is smaller than unity, then for larger values of v it becomes larger than unity, and eventually Z approaches unity from above. Lower figures: The functions dY/dx and dZ/dx as a function of v for the indicated values of $x = a/a_0$. The function dY/dx never changes sign, while the function dZ/dx does. Note that for $x^{-1} = 1100$, the values of dY/dx and dZ/dx have been multiplied by 10^{-3} .

III. LEMAÎTRE–TOLMAN–BONDI MODELS AS A PERTURBED CONFORMAL POISSON METRIC

The LTB model of the previous section is an example of a nonlinear cosmological model. It is also a model that exhibits an observable that is very different from the unperturbed model (EdS). Our goal now is to investigate where and why the “no-go” argument discussed in the Introduction fails.

To get insights, we will express the LTB metric, Eq. (4), in the form of a perturbed conformal Poisson metric with small potentials. We will consider a metric perturbed about the EdS (spatially flat) background. In the metric we

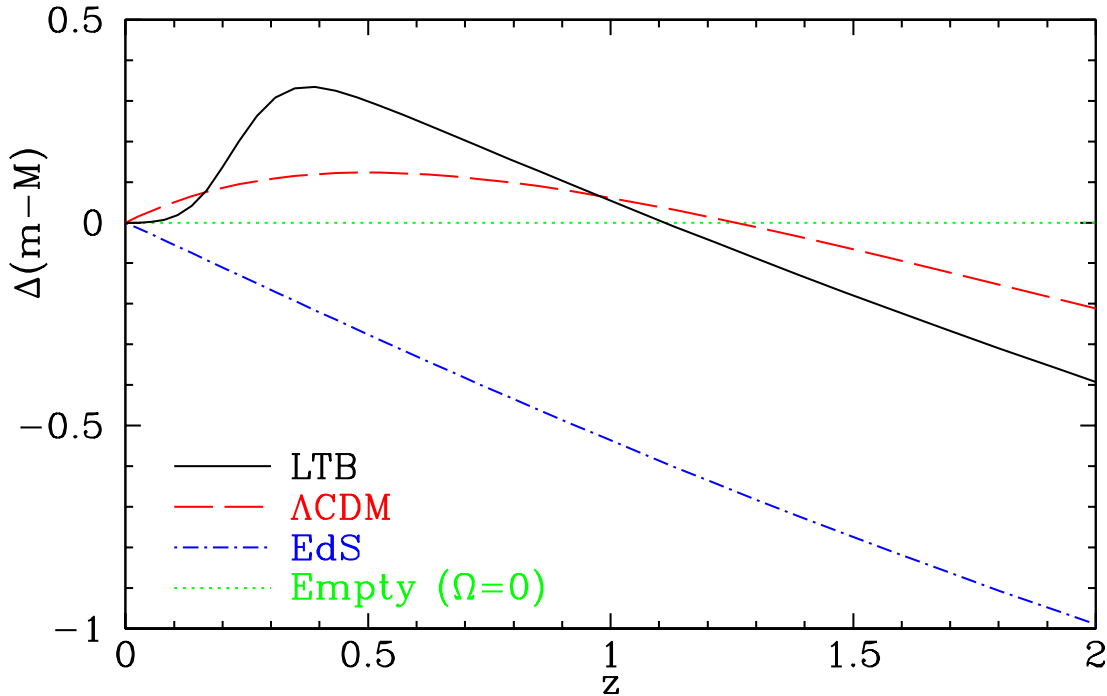


FIG. 3: The luminosity distance as a function of redshift. The curve labeled LTB is the LTB model of this paper, the model labeled Λ CDM is the standard Λ CDM model with $\Omega_\Lambda = 0.7$, the model labeled EdS is the EdS model, and the model labeled Empty is an empty universe model. Rather than $H_0 d_L(z)$, we show the usual difference in the distance modulus compared to the empty model.

adopt, vector and tensor perturbations are absent: the perturbations are given by the potentials ψ and ϕ ,⁷

$$ds^2 = a^2(\tau) \left[-(1 + 2\psi)d\tau^2 + (1 - 2\phi)dr^2 + (1 - 2\phi)r^2 d\Omega^2 \right], \quad (19)$$

where τ is conformal time, $ad\tau = dt$.

When considering a dust model (or, in general, in the absence of anisotropic stress), one usually takes the same scalar perturbation in both the spatial and temporal part of the metric, that is, $\psi = \phi$. Also, it is usually assumed that the potentials are time independent.

As we will soon show, however, we will have to allow the two potentials to differ and be time dependent: this is caused directly by the nonlinear structure of the LTB model. This can be seen mathematically by the fact that in the case $\psi(r) = \phi(r)$, the system of equations will be overconstrained if we are beyond linear order. The cause of why $\psi \neq \phi$ and they are time dependent is actually one of the main issues we will try to understand in this paper: what we want to show is that it is not possible to describe the AAG model by means of the perturbed conformal Newtonian metric of Eq. (1) as far as the linearized theory is concerned.

Of course, this behavior is due to the fact that the AAG model has an initial density and curvature perturbation which is not within the linear regime of perturbation theory. Even though this is the specific cause of the particular behavior of the AAG model, we will try to learn the general physical cause of that behavior. The AAG model will be just a tool to understand the general lesson about the importance of voids not dynamically restricted which, as we will explain, are a key-feature to evade the no-go argument discussed in the Introduction.

⁷ The perturbed conformal Poisson metric is closely related to the perturbed conformal Newtonian metric of Eq. (1). The differences are that in the perturbed conformal Poisson metric the spatial perturbation (ϕ) need not equal the temporal perturbation (ψ), and the perturbed conformal Newtonian metric also has the additional restrictions on the metric coefficients discussed after Eq. (1).

We point out that the calculations we are going to show are consistent with the standard result that at linear order the potentials are time-independent and identical: $\psi(r) = \phi(r)$. It is indeed possible to show (see Ref. [20]) that if there is no time dependence, then the equations will not overconstrain the scalar potentials in the case $\psi = \phi$.

In the next subsection we will set up the gauge transformation needed to calculate the potentials ψ and ϕ of the metric of Eq. (19) in the perturbed conformal Poisson metric corresponding to the LTB metric of Eq. (4) in the synchronous gauge.

A. Gauge transformation

To be able to compare the metrics of Eqs. (4) and (19), we will express the latter in the synchronous gauge. We will use the gauge transformations of the linearized theory: the consistency of this will be discussed later.

The generic form of the perturbed EdS model, both in Cartesian and spherical coordinates, is [33]

$$\begin{aligned} ds^2 &= a^2(\tau) \left\{ -(1+2\psi)d\tau^2 - 2\partial_i\omega dx^i d\tau + [(1-2\phi)\delta_{ij} + D_{ij}\chi] dx^i dx^j \right\} \\ &= a^2(\tau) \left[-(1+2\psi)d\tau^2 - 2\omega' dr d\tau + \left(1-2\phi + \frac{2}{3}\Upsilon\right) dr^2 + \left(1-2\phi - \frac{1}{3}\Upsilon\right) r^2 d\Omega^2 \right], \end{aligned} \quad (20)$$

where $D_{ij} = \partial_i\partial_j - \frac{1}{3}\delta_{ij}\nabla^2$ and $\Upsilon = \chi'' - \chi'/r$. Because of spherical symmetry we are including only longitudinal degrees of freedom in the metric perturbations.

Under a gauge transformation the metric perturbations transform according to

$$\tilde{\psi} = \psi - \partial_\tau\zeta - \frac{\partial_\tau a}{a}\zeta \quad (21)$$

$$\tilde{\omega} = \omega + \zeta + \partial_\tau\beta \quad (22)$$

$$\tilde{\phi} = \phi - \frac{1}{3}\nabla^2\beta + \frac{\partial_\tau a}{a}\zeta \quad (23)$$

$$\tilde{\chi} = \chi + 2\beta, \quad (24)$$

where ζ and β express the gauge freedom. In radial coordinates, $\nabla^2\beta = \beta'' + 2\beta'/r$. This transformation corresponds to a diffeomorphism which keeps the perturbations in Eq. (20) small: this is actually the definition of gauge transformations in the linearized theory. The new coordinates are given by

$$\begin{aligned} \tilde{\tau} &= \tau + \zeta \\ \tilde{\vec{x}} &= \vec{x} - \vec{\nabla}\beta \\ \tilde{r} &= r - \beta', \end{aligned} \quad (25)$$

where again only the longitudinal component has been taken into account.⁸

In the following, $\tilde{\psi}, \tilde{\omega}, \tilde{\phi}, \tilde{\chi}, \tilde{\tau}, \tilde{\vec{x}},$ and \tilde{r} will refer to the quantities in the LTB synchronous gauge, while the corresponding quantities without the tilde will refer to quantities in the perturbed conformal Poisson metric.

We can now choose the gauge transformations in order to end up with $\tilde{\psi} = \tilde{\omega} = 0$, that is, to end up in the synchronous gauge. Taking in account that we are coming from a metric of the form Eq. (19), which has $\omega = 0$ and $\psi \neq 0$, we find from Eqs. (21) and (22) that

$$\tilde{\psi} = 0 \rightarrow \psi = \partial_\tau\zeta + \frac{\partial_\tau a}{a}\zeta = (a\zeta)' \quad (26)$$

$$\tilde{\omega} = 0 \rightarrow \zeta = -\partial_\tau\beta = -a\dot{\beta}. \quad (27)$$

These expressions can be expressed in integral form as

$$\zeta(r, t) = \frac{1}{a(t)} \int_{\bar{t}}^t \psi(r, t_1) dt_1 + \frac{\bar{a}}{a(t)} \bar{\zeta}(r) \quad (28)$$

$$\beta(r, t) = - \int_{\bar{t}}^t \frac{dt_2}{a^2(t_2)} \int_{\bar{t}}^{t_2} \psi(r, t_1) dt_1 - 3\bar{\zeta}(r) \frac{\bar{t}}{a} \left(1 - \frac{\bar{t}^{1/3}}{t^{1/3}}\right) + \bar{\beta}(r), \quad (29)$$

⁸ Only β' will appear in the equations since the displacement is $dr = -\beta'$.

where the overbar denotes the quantity evaluated at $t = \bar{t}$, the initial time of the evolution (\bar{t} corresponds to $x^{-1} = 1100$).

The time-independent integration functions $\bar{\zeta}(r)$ and $\bar{\beta}(r)$ express the residual gauge freedom, which we are going to discuss shortly. But before doing that, let us make use of the remaining two gauge transformations, Eqs. (23) and (24).

Comparing the LTB metric, Eq. (4), with the form of the perturbed metric, Eq. (20), we see

$$1 - 2\tilde{\phi} + \frac{2}{3}\tilde{\Upsilon} = \frac{R'^2}{a^2 W^2} \quad (30)$$

$$1 - 2\tilde{\phi} - \frac{1}{3}\tilde{\Upsilon} = \frac{R^2}{a^2 r^2}. \quad (31)$$

Now compare the perturbed conformal Poisson metric, Eq. (19), with the form of the perturbed metric, Eq. (20), with result that $\Upsilon = \chi'' - \chi'/r = 0$. The general solution to this equation is $\chi = C_1 r^2 + C_2$, where C_1 and C_2 are constant in r (but possibly time-dependent). In our case we are describing a model where $\chi \rightarrow 0$ as $r \rightarrow \infty$, *i.e.*, it approaches the unperturbed EdS solution at large r , so we must choose $C_1 = C_2 = \chi = 0$. Therefore $\Upsilon = 0$.

Since we know $\tilde{\phi}$ and $\tilde{\Upsilon}$, we can write

$$1 - 2\phi + 2\beta'' - \frac{4}{3}\frac{a}{t}\zeta = \frac{R'^2}{a^2 W^2} \quad (32)$$

$$1 - 2\phi + 2\frac{\beta'}{r} - \frac{4}{3}\frac{a}{t}\zeta = \frac{R^2}{a^2 r^2}. \quad (33)$$

Since we know ζ and β in terms of the potentials and initial data for ζ and β from Eqs. (28) and (29), we finally find the dynamical equations for the potentials $\psi(r, t)$ and $\phi(r, t)$:

$$\begin{aligned} 1 - 2\phi(r, t) - 2 \int_{\bar{t}}^t \frac{dt_2}{a^2(t_2)} \int_{\bar{t}}^{t_2} \psi''(r, t_1) dt_1 + 6\bar{\zeta}''(r) \frac{\bar{t}}{\bar{a}} \left(1 - \frac{\bar{t}^{1/3}}{t^{1/3}}\right) + 2\bar{\beta}''(r) - \frac{4}{3t} \int_{\bar{t}}^t \psi(r, t_1) dt_1 \\ - \frac{4}{3} \frac{\bar{a}}{t} \bar{\zeta}(r) = \frac{R'^2(r, t)}{a^2(t) W^2(r)} \end{aligned} \quad (34)$$

$$\begin{aligned} 1 - 2\phi(r, t) - 2 \int_{\bar{t}}^t \frac{dt_2}{a^2(t_2)} \int_{\bar{t}}^{t_2} \frac{\psi'(r, t_1)}{r} dt_1 + 6 \frac{\bar{\zeta}'(r)}{r} \frac{\bar{t}}{\bar{a}} \left(1 - \frac{\bar{t}^{1/3}}{t^{1/3}}\right) + 2 \frac{\bar{\beta}'(r)}{r} - \frac{4}{3t} \int_{\bar{t}}^t \psi(r, t_1) dt_1 \\ - \frac{4}{3} \frac{\bar{a}}{t} \bar{\zeta}(r) = \frac{R^2(r, t)}{r^2 a^2(t)}. \end{aligned} \quad (35)$$

These are the dynamical equations to solve for $\phi(r, t)$ and $\psi(r, t)$.

Before solving, it is illustrative to evaluate Eqs. (34) and (35) at the initial time $t = \bar{t}$ to find the integration functions $\bar{\zeta}(r)$ and $\bar{\beta}'(r)$. The result is

$$\bar{\zeta}(r) = -\frac{3}{2} \frac{\bar{t}}{\bar{a}} \left[\bar{\phi}(r) - \int_r^\infty \frac{W^2(r_1) - 1}{2r_1 W^2(r_1)} dr_1 \right] \quad (36)$$

$$\bar{\beta}'(r) = r \int_r^\infty \frac{W^2(r_1) - 1}{2r_1 W^2(r_1)} dr_1. \quad (37)$$

The fact that $\bar{\zeta}(\infty) = 0$ was used in Eq. (36): all the gauge quantities have to go to zero as $r \rightarrow \infty$ where the spacetime is exact Einstein-de Sitter.

The residual gauge freedom expressed by $\bar{\zeta}(r)$ and $\bar{\beta}'(r)$ is therefore fixed by the value of ϕ at initial time, that is, by the initial conditions of the hole in the synchronous gauge.

Note that β' must vanish at the center of the hole because of spherical symmetry. Only ζ is allowed to be nonzero at $r = 0$.

B. Potentials

With some manipulation we can express Eqs. (34) and (35) in a more manageable form. The difference of Eqs. (34) and (35) yields one equation, while combining Eq. (34) with Eq. (35) multiplied by r and then differentiated with respect to r yields a second equation:

$$\int_{\bar{t}}^t \frac{dt_1}{a^2(t_1)} \int_{\bar{t}}^{t_1} \left(\frac{\psi'(r, t_2)}{r} \right)' dt_2 + 3 \frac{\bar{t}}{\bar{a}} \left(1 - \frac{\bar{t}^{1/3}}{\bar{t}^{1/3}} \right) \left(\frac{\bar{\zeta}'(r)}{r} \right)' - \left(\frac{\bar{\beta}'(r)}{r} \right)' = V(r, t) \quad (38)$$

$$\phi'(r, t) + \frac{2}{3} \frac{1}{t} \int_{\bar{t}}^t \psi'(r, t_1) dt_1 + \frac{2}{3} \frac{\bar{a}}{t} \bar{\zeta}'(r) = S(r, t), \quad (39)$$

where the functions $V(r, t)$ and $S(r, t)$ are defined as

$$V(r, t) = \frac{1}{2r} \left(\frac{R^2(r, t)}{a^2(t)r^2} - \frac{R'^2(r, t)}{a^2(t)W^2(r)} \right) \quad (40)$$

$$S(r, t) = \frac{1}{2r} \left(\frac{R^2(r, t)}{a^2(t)r^2} + \frac{R'^2(r, t)}{a^2(t)W^2(r)} - \frac{2R(r, t)R'(r, t)}{a^2(t)r} \right). \quad (41)$$

Using the fact that as $r \rightarrow \infty$, the potentials and their derivatives must vanish, we can integrate Eqs. (38) and (39) with respect to r to obtain

$$\int_{\bar{t}}^t \frac{dt_1}{a^2(t_1)} \int_{\bar{t}}^{t_1} \psi(r, t_2) dt_2 + 3 \frac{\bar{t}}{\bar{a}} \left(1 - \frac{\bar{t}^{1/3}}{\bar{t}^{1/3}} \right) \bar{\zeta}(r) - \bar{\beta}(r) = \int_r^\infty dr_1 r_1 \int_{r_1}^\infty V(r_2, t) dr_2 \quad (42)$$

$$\phi + \frac{2}{3} \frac{1}{t} \int_{\bar{t}}^t \psi(r, t_1) dt_1 + \frac{2}{3} \frac{\bar{a}}{t} \bar{\zeta}(r) = - \int_r^\infty S(r_1, t) dr_1. \quad (43)$$

Final manipulations involving multiple differentiations with respect to t and integration by parts yield the results:

$$\psi(r, t) = \frac{1}{2} \int_r^\infty (r_1^2 - r^2) \dot{Q}(r_1, t) dr_1 \quad (44)$$

$$\phi(r, t) = -\frac{1}{2} \frac{\dot{a}}{a} \int_r^\infty (r_1^2 - r^2) Q(r_1, t) dr_1 - \int_r^\infty S(r_1, t) dr_1, \quad (45)$$

where $Q(r, t) = a^2(t) \dot{V}(r, t)$.

Note that the integration functions $\bar{\zeta}(r)$ and $\bar{\beta}(r)$ have disappeared from the final solution. They are, however, determined by the value of $\phi(r, \bar{t})$ at initial time as seen from Eqs. (36) and (37). For completeness we give the expressions for $\zeta(r)$ and $\beta'(r)$:

$$\zeta(r, t) = \tilde{\tau} - \tau = \frac{1}{2a} \int_r^\infty a^2(r_1^2 - r^2) \dot{V}(r_1, t) dr_1 \quad (46)$$

$$\beta'(r, t) = r - \tilde{r} = r \int_r^\infty V(r_1, t) dr_1. \quad (47)$$

Now we are in a position to express the potentials, the displacements in time, $\Delta t = a\zeta(r, t)$, and radial coordinate, $\Delta r = \beta'(r, t)$, in terms of the new radial coordinate $v \equiv H_0 a_0 r$. In terms of the variables Y and Z defined in Sec. II B, the expressions are

$$2\psi(v, x) = \int_v^\infty (v_1^2 - v^2) M(x, v_1) \frac{dv_1}{v_1} \quad (48)$$

$$2\phi(v, x) = - \int_v^\infty (v_1^2 - v^2) N(x, v_1) \frac{dv_1}{v_1} - \int_v^\infty P(x, v_1) \frac{dv_1}{v_1} \quad (49)$$

$$2 \frac{\Delta t}{t} = \frac{3}{2} \int_v^\infty (v_1^2 - v^2) N(x, v_1) \frac{dv_1}{v_1} \quad (50)$$

$$2 \frac{\Delta r}{r} = \int_v^\infty L(x, v_1) \frac{dv_1}{v_1}. \quad (51)$$

The functions $M(x, v)$, $N(x, v)$, $P(x, v)$, and $L(x, v)$ are

$$M(x, v) = x \left(\frac{dY(x, v)}{dx} \right)^2 - \frac{x}{W^2(v)} \left(\frac{dZ(x, v)}{dx} \right)^2 + \frac{Z^2(x, v)}{2xW^2(v)} \left(\frac{A_2(v)}{Y^2(x, v)Z(x, v)} - 2\frac{A_1(v)}{Y^3(x, v)} - 1 \right) - \frac{Y^2(x, v)}{2x} \left(\frac{A_1(v)}{Y^3(x, v)} - 1 \right) \quad (52)$$

$$N(x, v) = Y(x, v) \frac{dY(x, v)}{dx} - \frac{Z(x, v)}{W^2(v)} \frac{dZ(x, v)}{dx} \quad (53)$$

$$P(x, v) = Y^2(x, v) + \frac{Z^2(x, v)}{W^2(v)} - 2Y(x, v)Z(x, v) \quad (54)$$

$$L(x, v) = Y^2(x, v) - \frac{Z^2(x, v)}{W^2(v)}, \quad (55)$$

where, as before, $x = a/a_0$. The evolution equations for Y and Z are given in Eqs. (12). The initial conditions are $Y(v, \bar{x}) = Z(v, \bar{x}) = 1$ at $\bar{x}^{-1} = 1100$. It is clear that for an EdS solution ($W(v) = Y(v, x) = Z(v, x) = 1$, $A_1(v) = 1$, and $A_2(v) = 3$) the sources $M(x, v)$, $N(x, v)$, $P(x, v)$, and $L(x, v)$ vanish. Since we will never allow shell crossing in the evolution, each shell evolves separately.

In the next sections we will present the results for the potentials and coordinate displacements.

C. Results

First, we show in Fig. 4 the values of the potentials $\psi(x, v)$ and $\phi(x, v)$ for various values of $x = a_0/a$. There are several striking features. First of all, at the initial time, $x^{-1} = 1100$ (as well as for $x^{-1} = 500$), ϕ and ψ are greater than unity for $v \lesssim 0.3$. Also striking is the fact that near $v = 0$, $\phi \neq \psi$. For $x^{-1} \lesssim 100$, ϕ and ψ are smaller than unity, but they have different signs.

In the next section we will explain the reason for this behavior. Here, we note that when the potentials are greater than unity, they are constant within the horizon. If we take the initial epoch to be $x^{-1} = 1100$, then v_H is found by solving Eq. (16). The value of v_H for the LTB metric is not too much different than the corresponding value for the EdS model, $v_H = 2x^{1/2}$. In the EdS model, $v_H = 0.06, 0.09, 0.14, 0.20, 0.6, 1.15$, and 2 at $x^{-1} = 1100, 500, 200, 100, 10, 3$, and 1 respectively. In Fig. 4 we indicate values of v_H for $x^{-1} = 500$ and 200 . As seen in Fig. 4, when the potentials are larger than unity, within the scale of the horizon, they are very nearly constant. We will return to this point in Sect. V.

Now we turn to Fig. 5 where we show the coordinate differences between the LTB metric and the perturbed conformal Poisson metric. First, let us examine Δt . At the initial point in the evolution $\Delta t/t$ is much larger than unity and positive. So even at the very beginning of the calculation *we can not express the LTB metric in terms of a perturbed conformal Newtonian metric!* This occurs even though the metric is everywhere regular, and density perturbations are not highly nonlinear.

Eventually, when x drops below about $x^{-1} = 100$, $\Delta t/t$ becomes smaller than unity and continues to decrease. In the next section we will discuss the cause of this behavior.

Now let us turn to Δr . At the initial point in the evolution, $x^{-1} = 1100$, Δr is positive. This means that $r > \tilde{r}$, or the coordinate label in the perturbed conformal Poisson metric is greater than the coordinate label in the synchronous gauge. For other values of x , Δr is negative (*i.e.*, $r < \tilde{r}$, or the coordinate label in the perturbed conformal Poisson metric is less than the coordinate label in the synchronous gauge).

Finally, we turn to the issue of peculiar velocities. We first remark that the dust LTB metric of Eq. (4) is comoving: there are *no* peculiar velocities. Again denoting a quantity in the synchronous frame by a tilde, the four-velocity is $\tilde{u}^\mu = (1, \vec{0})$. However in the Poisson frame there are peculiar velocities (see also [34]). At linear order, under a coordinate transformation $\tilde{x}^\mu \rightarrow \tilde{x}^\mu - \epsilon^\mu$, we have (quantities in the Poisson frame do not carry a tilde):

$$u^\mu(x) = \tilde{u}^\mu(x) - \partial_\nu \epsilon^\mu \tilde{u}^\nu(x) + \epsilon^\sigma \partial_\sigma \tilde{u}^\mu(x) \quad (56)$$

$$u_\mu(x) = \tilde{u}_\mu(x) + \partial_\mu \epsilon^\nu \tilde{u}_\nu(x) + \epsilon^\sigma \partial_\sigma \tilde{u}_\mu(x). \quad (57)$$

From this we find (\hat{r} is a unit vector in the radial direction)

$$u^\mu(x) = (1 - a\dot{\zeta} - \dot{a}\zeta, \dot{\beta}'\hat{r}) = (1 - \psi, \dot{\beta}'\hat{r}) \quad (58)$$

$$u_\mu(x) = (-1 - a\dot{\zeta} + \dot{a}\zeta, a^2\dot{\beta}'\hat{r}) = (-1 - \psi, a^2\dot{\beta}'\hat{r}). \quad (59)$$

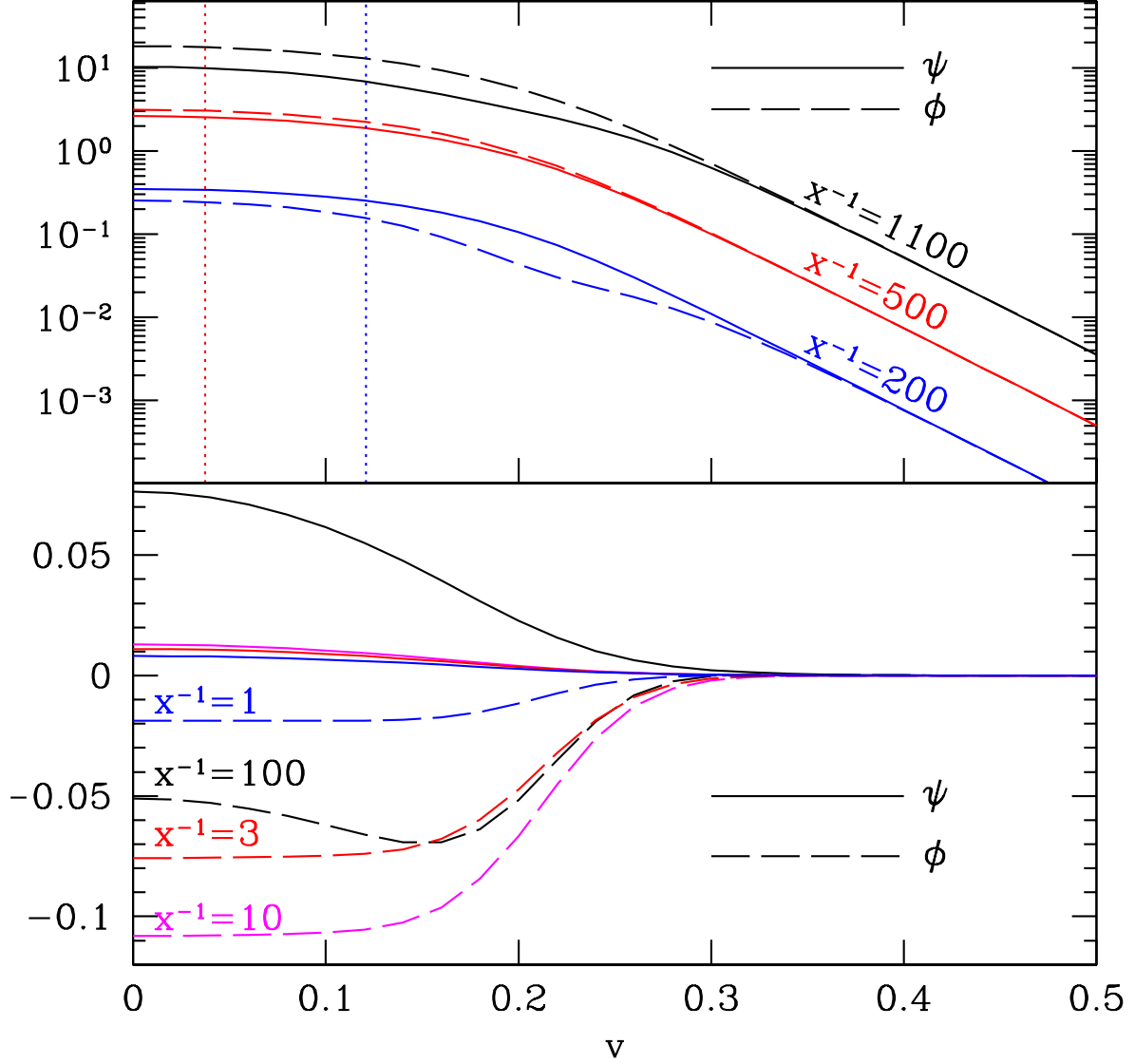


FIG. 4: The gauge potentials $\psi(x, v)$ and $\phi(x, v)$ as function of v for the indicated values of x . The potential $\psi(x, v)$ is indicated by solid curves and the potential $\phi(x, v)$ is indicated by dashed curves. In the lower half of the figure the values of x are indicated only for $\phi(x, v)$; the values of x for $\psi(x, v)$ are, from top to bottom, $x^{-1} = 100, 10, 3$, and 1 . In the upper half of the figure, the values of v at the horizon are indicated by a vertical dotted line for $x^{-1} = 500$ (leftmost line) and $x^{-1} = 200$.

As expected, the change in the four-velocities is of the same order as the gauge transformation. At linear order $u^\mu u_\mu = -1$ and $u_\mu = g_{\mu\nu} u^\nu$.

The value of u^r would be interpreted as a peculiar velocity. Now we express the four-velocity as $u^\mu = (\gamma, \gamma v^i)$. The three-velocity is $\vec{v} = \sqrt{h_{rr}} v^r \hat{r} = a v^r \hat{r}$ at linear order. Using this, $\gamma \vec{v} = a \dot{\beta}' \hat{r} = a \dot{\beta}' \hat{r}$, so

$$\gamma \vec{v} = a \dot{\beta}' \hat{r} = v x^{1/2} \int_{\tilde{v}}^{\infty} N \frac{d\tilde{v}}{\tilde{v}} \hat{r}. \quad (60)$$

The result for $\gamma \vec{v}$ as a function of $v = H_0 a_0 r$ is shown in Fig. 6 for several values of x . The large initial values of the velocity are the key to understanding why the perturbative description breaks down.

We now turn to the discussion.

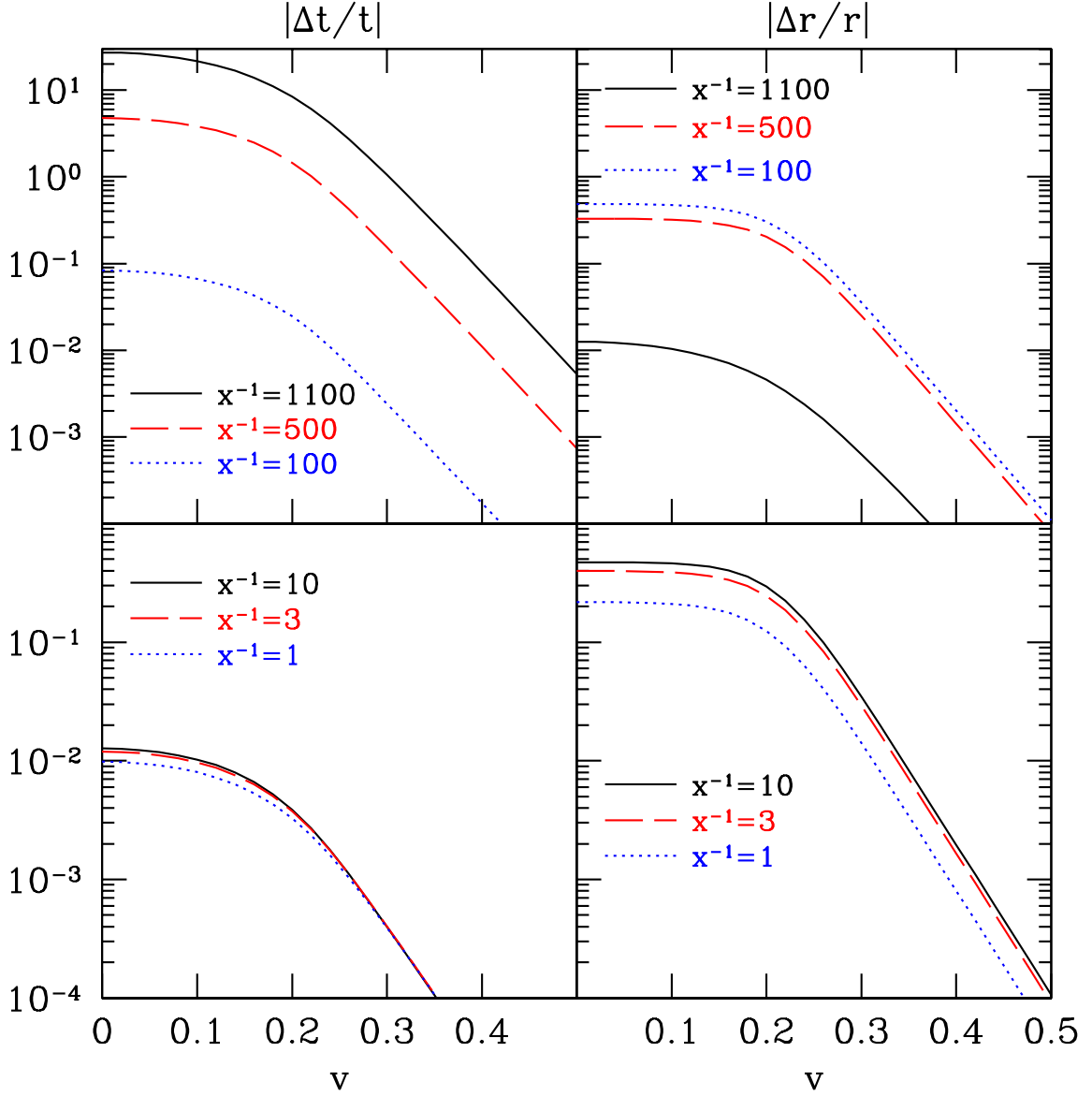


FIG. 5: The time displacement $\Delta t/t$ and coordinate displacement $\Delta r/r$ as a function of v for the indicated values of x . The time displacement Δt is negative for $x^{-1} = 1100, 500$, and 100 . It is positive for $x^{-1} = 10, 3$, and 1 . For $x^{-1} = 1100$, Δr is positive, for all other values of x , Δr is negative. Clearly, $\Delta r = r\Delta r/r$ vanishes in the limit $r \rightarrow 0$ as it must.

IV. DISCUSSION

The linear gauge transformation we have performed in the previous Section is a useful tool to understand where and why the no-go argument discussed in the Introduction fails. In this Section, first we will introduce the *general* physical cause of the breakdown of the description by means of the perturbed conformal Poisson metric. Then we will show how this general feature shows up in the model here examined. Finally we will conclude the Section with some comments about other models developed in the literature.

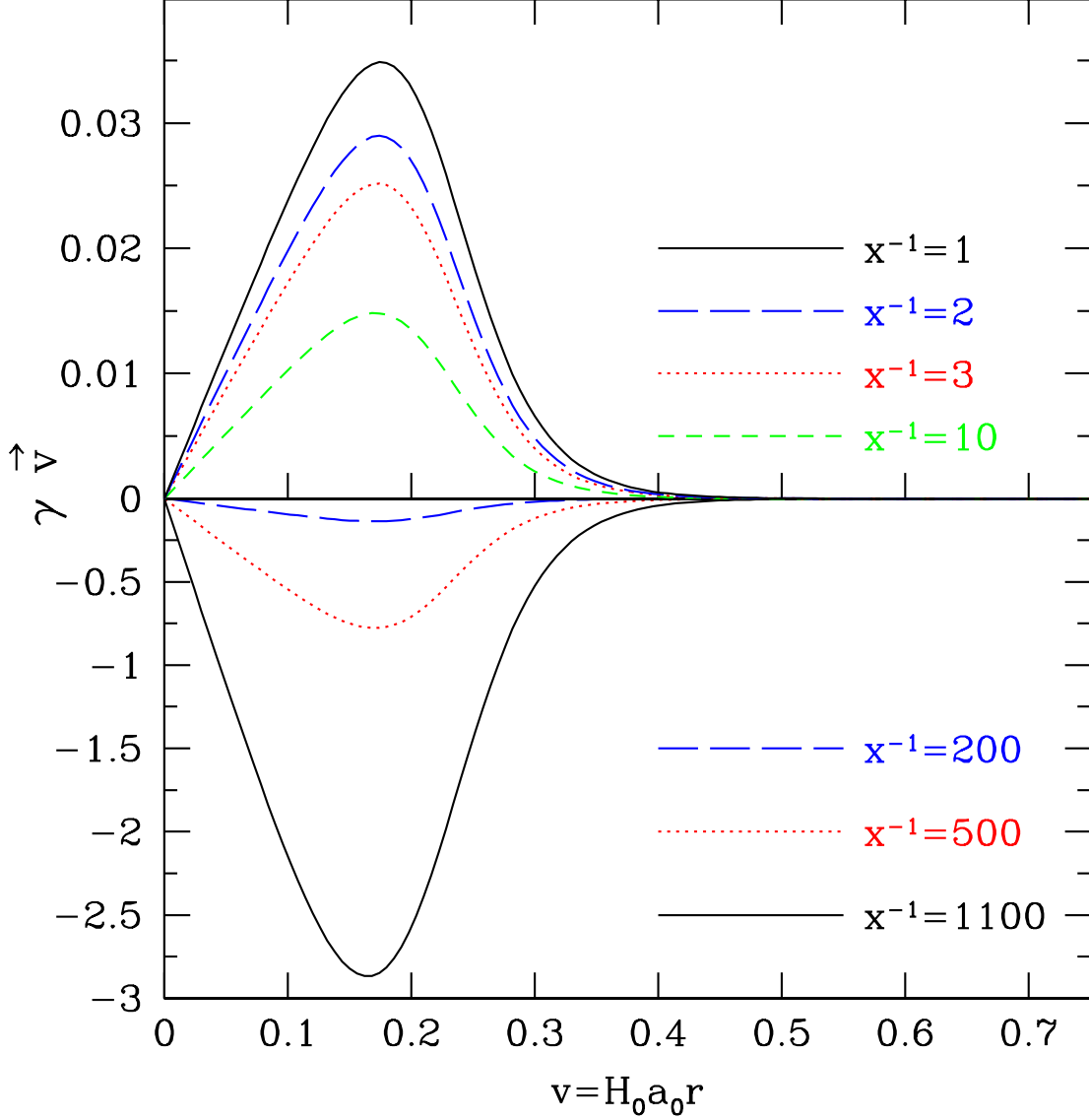


FIG. 6: The peculiar velocity in the Poisson frame as a function of $v = H_0 a_0 r$ for the indicated values of x . A negative (positive) value corresponds to a radial velocity towards (away from) the center.

A. Lack of a global background

The description by means of the perturbed conformal Poisson metric breaks down because of the large ΔH in the AAG model. As can be seen from Fig. 7,

$$\frac{\Delta H_{\perp,r}}{H_{\text{EdS}}} = \frac{H_{\perp,r} - H_{\text{EdS}}}{H_{\text{EdS}}} \quad (61)$$

is of order unity. A large ΔH is a typical feature of models with inhomogeneities, and from this point of view we think the LTB model is a useful tool to study the consequences of the evolution of structures in the real universe. In particular, the AAG version allows us to follow the evolution of the inhomogeneities for a rather large time span, thanks to the large initial infall velocity of the shells (negative value of $\Delta H/H_{\text{EdS}}$ for $x^{-1} = 1100$, as can be seen from Fig. 7).

A different expansion rate means a different FLRW solution, and even if the initial ΔH is small, the two solutions

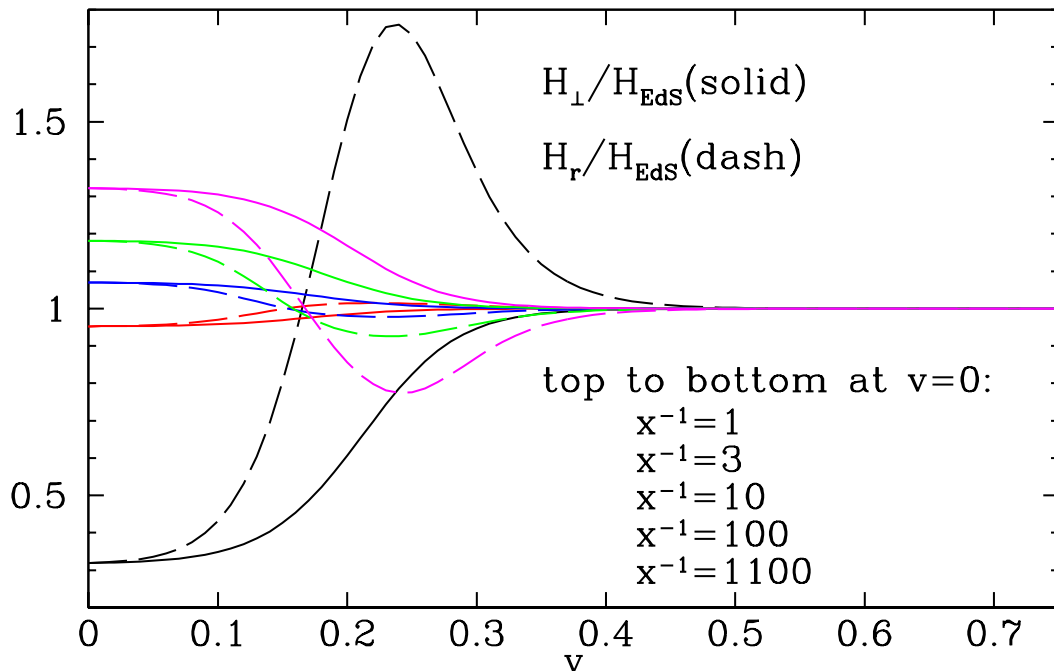


FIG. 7: The expansion rates as a function of v for the indicated values of x .

(void and EdS) will eventually follow very different evolutions. What we have in mind is the comparison of a background FLRW solution in the underdensity (the void region) and in the FLRW solution at large v . We will denote the value of v beyond which the solution is approximately EdS as v_{EdS} . We make the point that these two patches have different backgrounds, even though the “average” background *is* the EdS solution. The AAG model can indeed be thought of as an exact Swiss-cheese model matched to the density and the (zero) curvature of the EdS solution at a sufficiently large radius ($v \gtrsim v_{\text{EdS}}$). We can imagine populating the universe with other holes of radius $v \sim v_{\text{EdS}}$. On scales larger than any spherical hole, the AAG model evolves as the EdS model. From this perspective, in the framework developed by Buchert [35], the backreaction of the inhomogeneities is zero. (See Refs. [7, 16, 17] for a discussion.) Here, we find a lack of a global background in spite of the absence of a volume backreaction.

It can happen that at some specific time the background of the void patch is close to the EdS solution. This will be, however, a special moment because of the different evolution of the two patches. It will be more typical to have a large departure from the EdS flow, which will be manifest in a large ΔH or in large “peculiar” velocities. These “peculiar” velocities are the result of comparing the cosmic evolution of two different FLRW solutions, or, in other words, the results of perturbing about the wrong background.

Summarizing, *an inhomogeneous universe featuring voids cannot be studied by means of a global homogeneous background, and this holds even if the inhomogeneities do not affect, as it happens in a swiss-cheese model, the global evolution.*

B. Discussion of the results

What we have just discussed is clearly shown by the results obtained in the previous section. To understand them it is useful to focus on two key quantities.

First, it is possible to show (see the Appendix) that the value of ϕ at the origin has the following time dependence:

$$\phi_0 \propto - \left(\frac{a_v(t)}{a(t)} - 1 \right)^2, \quad (62)$$

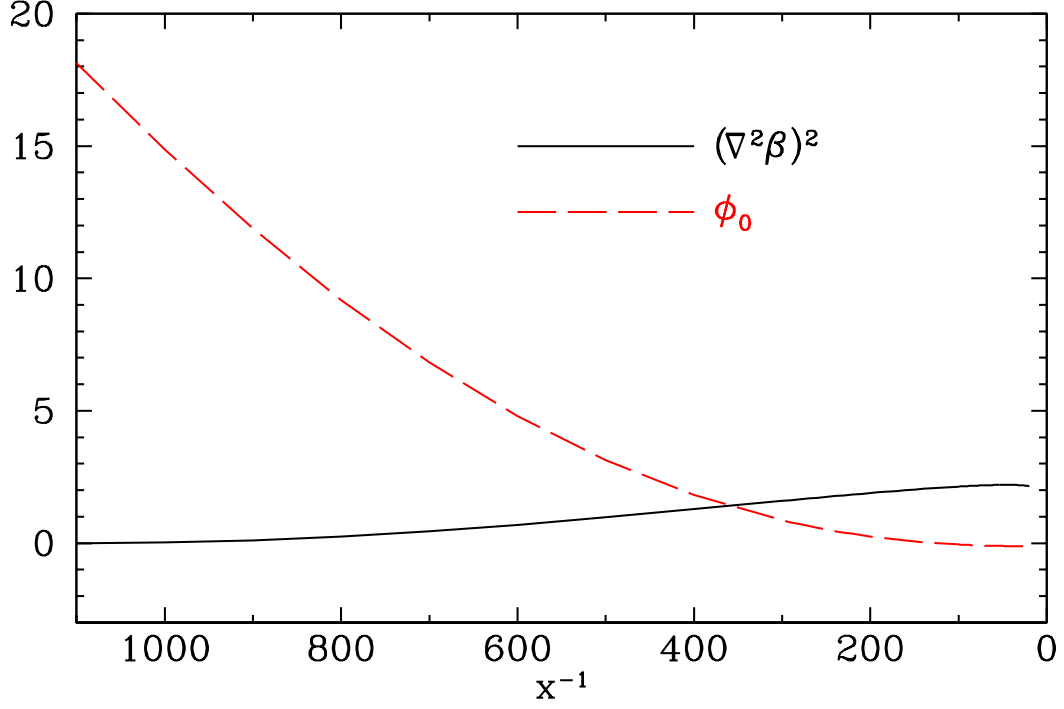


FIG. 8: The functions $(\nabla^2\beta)^2$ evaluated at $v = 0$ (dashed curve) and $\phi_0 = \phi(v = 0, x)$ (solid curve) as a function of $x^{-1} = a_0/a$.

where $a_v \equiv r^{-1} R|_{r=0}$ describes the scale factor of the void region. In turn, this implies that $\dot{\phi}_0 \propto \Delta H_\perp$. This expression makes clear that ϕ_0 can be thought as the time integral of ΔH .

A similar relation holds for β' (see the Appendix): $a\beta' \simeq R - ar$. This implies that $au^r = a\dot{\beta}' \simeq R\Delta H_\perp$, where we note that au^r , the velocity of the comoving matter in the Poisson frame shown in Fig. 6, is, as expected, almost the same as the “peculiar” velocity of the comoving matter with respect to the EdS background:

$$v_{pec} = \int_0^r dr_1 \frac{R'}{W} (H_r - H_{\text{EdS}}) \simeq R\Delta H_\perp = RH_{\text{EdS}} \frac{\Delta H_\perp}{H_{\text{EdS}}} \sim RH_{\text{EdS}}, \quad (63)$$

where the last relation holds because, as we have seen, $\Delta H/H$ is of order unity. (We have also used the fact that $W(r)$ is very close to unity.)

Expressing these key-quantities as a function of ΔH , which is the source of the effects, will help us in understanding the results of the previous section.

First, at early times ($x^{-1} \lesssim 500$) “peculiar” velocities are larger than c , as can be seen in Fig. 6. The reason can be understood from Eq. (63): at early times H_{EdS} is indeed large. This highlights the usefulness of the AAG model, which allows us to encompass both early times with a large expansion rate and the present time. This also illustrates the interesting fact that even with smaller ΔH we could have large peculiar velocities at early times when one might expect the system to be accurately described as a perturbation of an EdS universe. These large velocities cause the potentials to be greater than unity and the perturbed conformal Poisson metric to be unable to describe the metric in the void region. In the linear gauge transformation this shows up as the fact that peculiar velocities are of the same order as the gauge transformation. This is a general breakdown which affects the perturbed conformal Poisson metric even if we perform a nonlinear gauge transformation [36].

At later times, velocities become order $10^{-2}c$ as can be seen from Fig. 6; this is caused by the slowing down of the expansion. However, both $\beta' = \Delta r$ and ϕ do not depend on ΔH , but rather on its time integral, or, in other words, on the different size of the void region compared to the EdS region, that is, on $R - ar$. This dependence appears in ϕ because it is the spatial perturbation that has to connect these two differently expanding spatial regions. The reason for the breakdown of the linear transformation is, therefore, the growth of $\beta' = \Delta r$, that is, the departure of the two

metrics. This shows up directly in ϕ . The basic problem is that the linear gauge transformation neglects terms like $(\nabla^2\beta)^2$ compared to terms like ϕ : see Eq. (23). As you can see from Fig. 8, this approximation is no longer valid for $x^{-1} \lesssim 400$. So even if the velocities are small, the linear transformation breaks down because their time-integrated effect is large. As a consequence we find, for example, $\phi \neq \psi$. It is however possible to describe the late evolution of the model in the perturbed conformal Newtonian metric by means of a nonlinear gauge transformation whose potential follows nonlinear equations of motion [36].

C. Comments

We will comment now on the models of Refs. [37] and [38]. According to Ref. [37] there is no breakdown of the perturbed conformal Newtonian metric during the dynamical evolution of the *particular* (it is important to not generalize) LTB model the authors have considered. The model of Ref. [38] does not deal with the possibility of using the perturbed conformal Newtonian metric to describe the spacetime of the universe, but it will nevertheless help us to make our point because it is a model which can be described with the perturbed conformal Newtonian metric if we perform a nonlinear gauge transformation.

We start noting that in both Ref. [37] and Ref. [38] the validity of the perturbed conformal Newtonian metric is assumed as a starting point. These particular models are not allowed to have large peculiar velocities. The point is that this is a particular choice, and, in our opinion, not general as demonstrated by the dependence in Eq. (63) of the peculiar velocities on ΔH . We would like to stress again that these “background” peculiar velocities have nothing to do with anything that can be measured as a local effect. Therefore, the models of Refs. [37] and [38] over-restrict the dynamics of the inhomogeneities, or, equivalently, demand the existence of a global background. For example, in the model of Ref. [37], the initial ΔH of Eq. (63) is exactly zero, and in the model of Ref. [38] it is $\Delta H/H_{EdS} < 10^{-3}$. Therefore, these models serve as an illustration to show the circular reasoning at the basis of the no-go argument: if we demand that the spacetime metric of the inhomogeneous universe has a global background without any departure due to differently evolving regions, then we will find the validity of the perturbed conformal Newtonian metric. This is the main point of this work, and the linear gauge transformation is a useful tool to understand it.

It is interesting to note that the model of Ref. [38] can confront the SNe data, but its luminosity distance does not show a big departure in shape from the EdS one, while the AAG model features a luminosity distance similar to the Λ CDM model. This is mainly due to the size of the hole, roughly 10 times smaller than the AAG one. We point out that if we want to have a Λ CDM-like luminosity distance in a setup with only one hole and the observer at the center, then we will likely have large background peculiar velocities. This might, however, be a typical, but not a general feature. To illustrate this we have calculated the luminosity distance for the model of Ref. [38], but with a hole roughly 10 times larger: we found that $d\Delta(m - M)/dz < 0$ always. This can be seen, again, as due to a restriction on the dynamics: allowing larger peculiar velocities we find voids with more general dynamics. We stress again the usefulness of the AAG model in showing these general features.

V. CONCLUSIONS

The LTB model analyzed in this paper is a very useful toy model to explore the role of large inhomogeneities in the determination of cosmological observables such as the luminosity distance as a function of redshift. We employed the toy model to demonstrate where and why the no-go argument discussed in the Introduction fails. To this end we have performed a linear gauge transformation in order to understand the problems we have to face if we want to express the LTB model in the form of a perturbed conformal Newtonian metric, Eq. (1).

We would like to stress that we regard the AAG model as a tool useful to show a general feature needed to evade the no-go argument: we focused on the *general* physical cause of the nonlinear behavior of the AAG model more than on its particular initial conditions.

We came to the conclusion that the way the no-go argument is proved is by assuming, as a starting point, the validity of the argument itself. The way to escape the no-go argument is by allowing large “background peculiar velocities,” where these velocities have nothing to do with, *e.g.*, velocity dispersions in clusters or anything that can be measured as a local effect. If indeed inhomogeneities are responsible for the “apparent” acceleration of the universe, then the evolution of the expansion rate must resemble a Λ CDM model. If that is true, then there will naturally be “peculiar” velocities if one describes the evolution in terms of perturbations of an EdS model. One cannot simply assume peculiar velocities are small and then use that as a basis to show inhomogeneities can have no effect. In the calculation of peculiar velocities it is necessary to specify a background solution about which to calculate velocities. The peculiar velocities can be small in the Λ CDM background but not in the EdS background. The velocities appear

as a departure from EdS of the Hubble flow, preventing the metric from being written in the conformal Newtonian form.

In other words, to evade the no-go argument we need to free the inhomogeneous models of dynamical restrictions (small background peculiar velocities) which impose the existence of a global background.

Another way to see how the no-go argument of Eq. (1) fails is through the equations of motion: in order to have a model, *e.g.*, an LTB model, explain the observed departure of $d_L(z)$ from the EdS result requires nonlinear equations of motion, and this is because of the large background peculiar velocities which can generally occur. By this, we mean that in order to end up with a large spatial variation of the background H requires a nonlinear evolution like the one of the LTB model discussed in this paper. And this can occur even if it is possible, as in the AAG model, to describe an inhomogeneous universe by means of the perturbed conformal Newtonian metric from (let's say) $z = 2$ to present time. This is shown here by explicit calculation.

Therefore, one must reconsider very carefully the statement that inhomogeneities can not have a significant effect on cosmological observables such as the luminosity distance as a function of redshift if arguments are based on the *assumption* that the metric describing our universe can be written in the perturbed conformal Newtonian form of Eq. (1).

Now we enumerate some of our findings.

1. In the model we consider, even at late times when the density contrast is linear and the velocities are small, one can not express the LTB metric in the perturbed conformal Newtonian form of Eq. (1) by means of a linear gauge transformation. The breakdown of the linear transformation clearly shows the importance of background velocities.

The linear gauge transformation breaks down mainly because of the large $\Delta r = \beta'$. This is caused by the different expansion rates (ΔH) of the void and the EdS solution, as can be seen in Fig. 7, which shows the expansion rates as a function of v for several values of x . The result is that the two metrics do not remain close enough for a linear transformation to connect them. As discussed in the previous section, the basic problem is that the linear gauge transformation neglects terms like $(\nabla^2 \beta)^2$ compared to terms like ϕ . Summarizing, the cause of the break down of the linear gauge transformation is the large ΔH , and the underlying cause of that is the nonlinearity of the equations of motion. The failure described above can be stated as the fact that the linearized equations of motion work only for a limited range of times.

2. It is possible to find a nonlinear gauge transformation to overcome this problem with a perturbed conformal Newtonian metric description of the LTB metric whose potential follows nonlinear equations [36]. These nonlinear equations (which are actually the exact Einstein equations) at some time will typically give large potentials and make the perturbed conformal Newtonian gauge description inconsistent (large $\Delta t = a\zeta$ in the LTB model examined) because at some point the peculiar velocities will be larger than c if we do not restrict the dynamics, as shown by the AAG model.
3. Although at the present time, in the model we consider, the magnitude of the potentials are small, they are not equal at the level of the linearized theory, *viz.* $\psi \neq \phi$. This could naïvely be interpreted as some anisotropic stress or something else funny with the stress tensor. This is exactly the point that has been made in, *e.g.*, Ref. [3]: Analyzing an inhomogeneous model in the framework of a homogeneous model introduces spurious components and behavior to the stress tensor (*possibly even a negative-pressure fluid!*).
4. If we start with a perturbed EdS model, then the growth of perturbations will lead to the formation of large voids, filamentary structure, and other nonlinearities. Perhaps the LTB models are useful toy models to study the effect of that phenomenon. The model explored in this paper is a good example because it is capable of dealing with nonlinearities within a large timespan.
5. Finally, another point worth mentioning is the physical nature of super-Hubble modes of ϕ and ψ . At the initial time, within each Hubble radius patch, ϕ and ψ are very nearly constant, but possibly larger than one (with a value of about 20 near the origin). That *does not* mean that we can simply subtract different values, because we are only allowed to do this once. If we do it at $x^{-1} = 1100$, then at $x^{-1} = 1$ we would have ϕ and ψ near the origin of -20 .

Summarizing, inhomogeneities, in particular voids not dynamically restricted, undermine the existence of a global background.

The interesting question for future consideration is if backreactions⁹ of cosmological perturbations can substantially distort derived conclusions about the energy-momentum tensor of the universe without allowing dramatic violations of *statistical* homogeneity. The present work addresses the key issue that backreaction effects cannot be assumed *in principle* to be small on the basis of the no-go argument explained in the Introduction and therefore opens a wide range of possibilities to tackle the study of the inhomogeneities in the universe.

Acknowledgments

It is a pleasure to thank J. M. Bardeen, T. Buchert, S. M. Carroll, K. Van Acoleyen and H. Van Elst for useful discussions, comments and suggestions. This work was supported in part by the Department of Energy. V.M. would like to acknowledge the Kavli Institute for Cosmological Physics for hosting a visit to the University of Chicago and “Fondazione Angelo Della Riccia” for support. S.M. and V.M. acknowledge ASI contract I/016/07/0 “COFIS” for partial financial support.

APPENDIX: DETAILS OF THE APPROXIMATIONS USED IN SECT. IV

In this Appendix we will discuss the approximations used in Sect. IV. Although we have checked numerically that they hold, we will present here an analytic explanation.

1. Approximations for ϕ_0

We first want to motivate that the time dependence of ϕ near the origin can be estimated as $\phi_0 \sim -(a_v/a - 1)^2$, where $a_v = r^{-1} R|_{r=0}$, as used in Eq. (62).

The second term dominates the expression for $\phi(r, t)$ in Eqs. (45) or (49), so in the limit that $W(r) = 1$, $\phi_0(t)$ can be written as

$$\phi_0(t) \simeq - \int_0^{r_{\text{EdS}}} \frac{1}{2} \left(\frac{R}{a r_1} - \frac{R'}{a} \right)^2 \frac{dr_1}{r_1} = - \int_0^{r_{\text{EdS}}} \left[\left(\frac{R}{a r_1} - 1 \right)' \right]^2 \frac{r_1}{2} dr_1, \quad (\text{A.1})$$

where we defined r_{EdS} as the coordinate radius at which the metric is the EdS one (it will disappear from the final expression). To proceed further, define a function $c(r, t)$ as

$$\phi_0(t) = - \int_0^{r_{\text{EdS}}} \left[\left(\frac{R}{a r_1} - 1 \right)' \right]^2 \frac{r_1}{2} dr_1 = -c(0, t) \left[\int_0^{r_{\text{EdS}}} \left(\frac{R}{a r_1} - 1 \right)' \frac{r_1}{2} dr_1 \right]^2 \left[\int_0^{r_{\text{EdS}}} \frac{r_1}{2} dr_1 \right]^{-1}. \quad (\text{A.2})$$

Now define $R|_{r=0} = a_v r$ where a_v gives the scale factor for the FLRW solution at the center. Thanks to Birkhoff’s theorem, outer shells do not influence the center, which can be indeed thought as a homogeneous patch. Expanding $R(r, t)$ in the void region as¹⁰

$$\frac{R(r, t)}{r} = a_v(t) + a_{v2}(t) r^2 + \mathcal{O}(r^3), \quad (\text{A.3})$$

we find

$$\phi_0(t) \sim - \left(\frac{a_v}{a} - 1 \right)^2, \quad (\text{A.4})$$

⁹ We do not really distinguish between weak or strong backreaction because we think that what matters are the observables. Assuming, indeed, that an inhomogeneous model gives a Λ CDM-like luminosity distance, then it is not straightforward to understand which category of backreaction (weak or strong) the model belongs to. The strong backreaction indeed is about a change of background, but this is also the case for the weak backreaction because, as in the case of this example, it “defines” an effective background, the Λ CDM model. Moreover, the change of background of the strong backreaction should be related to observable data on the light cone as it is for the weak backreaction.

¹⁰ In the expansion $a_{v1} = 0$, thanks to the fact that $\rho'(0, t) = 0$ as discussed in Ref. [12].

where, after integrating by parts, we have made the approximation that the void region occupies almost all of the volume of the hole of radius r_{EdS} .

Now we wish to show that $c(r, t)$ depends only weakly on time. To this end, we expand $(R/ar)'$ and $[(R/ar)']^2$ in r around r_{EdS} to third order, that is up to the fourth derivative of R with respect to r , and then we plug the resulting series in the integrals. The result is

$$c(r, t) \simeq \frac{4}{3} + \frac{1}{9} \left(-\frac{4}{r_{\text{EdS}}} + \frac{R'''(r_{\text{EdS}}, t)}{R''(r_{\text{EdS}}, t)} \right) (r - r_{\text{EdS}}). \quad (\text{A.5})$$

The first remark is that the term proportional to $R'''(r_{\text{EdS}}, t)$ cancels. The dependence on time is therefore in the $R'''(r_{\text{EdS}}, t)/R''(r_{\text{EdS}}, t)$ term. Following a procedure similar to this one used to obtain Eq. (3.5) of Ref. [15], but keeping both density and curvature inhomogeneities, we find:

$$\frac{R'''(r_{\text{EdS}}, t)}{R''(r_{\text{EdS}}, t)} = \frac{3}{r_{\text{EdS}}} + \frac{d'''(r_{\text{EdS}})}{d''(r_{\text{EdS}})}, \quad (\text{A.6})$$

where $d(r) = \bar{\rho}(r, \bar{t}) + \bar{d}\rho(t)^{-1/3}k(r)$, \bar{d} is a constant, $\rho(t)$ is the EdS density, and $\bar{\rho}(r, \bar{t}) = 3\alpha(r)/8\pi R^3(r, \bar{t})$ is the initial averaged density. We see, therefore, that a general condition to have the constancy of $R'''(r_{\text{EdS}}, t)/R''(r_{\text{EdS}}, t)$ is that the second and third derivatives with respect to r of $\bar{\rho}(r, \bar{t})$ and $k(r)$ are proportional, so that the time dependence cancels. This is indeed the case in the AAG model. We remark that $\bar{\rho}(r, \bar{t})$ and $k(r)$ can be seen as the defining functions for a LTB model, and this result holds thanks to the matching guaranteed by $d'(r_{\text{EdS}}) = 0$.

2. Approximations for β'

We now discuss the approximation that $a\beta' \simeq R - ar$. Starting from Eq. (47), with the approximation that $W \simeq 1$, we have

$$\frac{\beta'(r, t)}{r} \simeq \int_r^\infty \frac{dr_1}{r_1} \left(\frac{R}{ar_1} - \frac{R'}{a} \right) \frac{1}{2} \left(\frac{R}{ar_1} + \frac{R'}{a} \right) = - \int_r^\infty dr_1 \left(\frac{R}{ar_1} \right)' \left[\frac{1}{2} \left(\frac{R}{ar_1} + \frac{R'}{a} \right) \right]. \quad (\text{A.7})$$

Now from Fig. 2, the term in the square brackets oscillates about one, so it is not a bad approximation to set it to unity. The integral can then be done with the result that $a\beta' \simeq R - ar$, used in Sect. IV.

-
- [1] A. Ishibashi and R. M. Wald, *Class. Quant. Grav.* **23**, 235 (2006).
 - [2] A. Gruzinov, M. Kleban, M. Porrati and M. Redi, *JCAP* **0612**, 001 (2006).
 - [3] E. W. Kolb, S. Matarrese and A. Riotto, *New J. Phys.* **8**, 322 (2006).
 - [4] G. Lemaitre, *Gen. Rel. Grav.* **29**, 641 (1997) [*Annales Soc. Sci. Brux. Ser. I Sci. Math. Astron. Phys. A* **53**, 51 (1933)].
 - [5] R. C. Tolman, *Proc. Nat. Acad. Sci.* **20**, 169 (1934).
 - [6] H. Bondi, *Mon. Not. Roy. Astron. Soc.* **107**, 410 (1947).
 - [7] V. Marra, E. W. Kolb, S. Matarrese and A. Riotto, *Phys. Rev. D* **76**, 123004 (2007).
 - [8] N. Mustapha, C. Hellaby and G. F. R. Ellis, *Mon. Not. Roy. Astron. Soc.* **292**, 817 (1997).
 - [9] M. N. Celerier, *Astron. Astrophys.* **353**, 63 (2000).
 - [10] H. Iguchi, T. Nakamura and K. i. Nakao, *Prog. Theor. Phys.* **108**, 809 (2002).
 - [11] P. S. Apostolopoulos, N. Brouzakis, N. Tetrads and E. Tzavara, *JCAP* **0606**, 009 (2006).
 - [12] R. A. Vanderveld, E. E. Flanagan and I. Wasserman, *Phys. Rev. D* **74**, 023506 (2006).
 - [13] D. J. H. Chung and A. E. Romano, *Phys. Rev. D* **74**, 103507 (2006).
 - [14] K. Enqvist and T. Mattsson, *JCAP* **0702**, 019 (2007).
 - [15] T. Biswas, R. Mansouri and A. Notari, *JCAP* **0712**, 017 (2007).
 - [16] V. Marra, E. W. Kolb and S. Matarrese, *Phys. Rev. D* **77**, 023003 (2008).
 - [17] V. Marra, arXiv:0805.4233 [astro-ph].
 - [18] V. Marra, arXiv:0803.3152 [astro-ph].
 - [19] N. Brouzakis, N. Tetrads and E. Tzavara, *JCAP* **0804**, 008 (2008).
 - [20] T. Biswas and A. Notari, *JCAP* **0806**, 021 (2008).
 - [21] N. Brouzakis and N. Tetrads, *Phys. Lett. B* **665**, 344 (2008).
 - [22] H. Alnes, M. Amarzguoui and Ø. Grøn, *Phys. Rev. D* **73**, 083519 (2006).
 - [23] H. Alnes and M. Amarzguoui, *Phys. Rev. D* **75**, 023506 (2007).
 - [24] J. Garcia-Bellido and T. Haugboelle, *JCAP* **0804**, 003 (2008).

- [25] A. G. Riess *et al.* [Supernova Search Team Collaboration], *Astrophys. J.* **607**, 665 (2004).
- [26] A. Notari, *Mod. Phys. Lett. A* **21**, 2997 (2006).
- [27] S. Rasanen, *JCAP* **0611**, 003 (2006).
- [28] T. Mattsson, arXiv:0711.4264 [astro-ph].
- [29] D. L. Wiltshire, arXiv:0712.3984 [astro-ph].
- [30] A. Paranjape and T. P. Singh, *Gen. Rel. Grav.* **40**, 139 (2008).
- [31] G. F. R. Ellis and T. Buchert, *Phys. Lett. A* **347**, 38 (2005).
- [32] G. F. R. Ellis, Relativistic cosmology – its nature, aims and problems. In *General Relativity and Gravitation* (D. Reidel Publishing Co., Dordrecht), ed. B. Bertotti, F. de Felice and A. Pascolini, pp. 215–288 (1984).
- [33] C. P. Ma and E. Bertschinger, *Astrophys. J.* **455**, 7 (1995).
- [34] G. F. R. Ellis, H. van Elst and R. Maartens, *Class. Quant. Grav.* **18**, 5115 (2001).
- [35] T. Buchert, *Gen. Rel. Grav.* **40**, 467 (2008).
- [36] K. Van Acoleyen, *JCAP* **0810**, 028 (2008).
- [37] A. Paranjape and T. P. Singh, *JCAP* **0803**, 023 (2008).
- [38] S. Alexander, T. Biswas, A. Notari and D. Vaid, arXiv:0712.0370 [astro-ph].